Academic Science Journal

Fabrication of some Quaternary Spinel Structure Electrodes for Photoelectrochemical Applications

Abdulsalam M. Hasan[1*], Ziad T. Khodair[2], Amar H. Jareeze Al-Keisy[3]

[1]The General Directorate for Education of Diyala

[2]Department of physics, College of Sciences, University of Diyala

[3]Nanotechnology and advanced materials research center, University of Technology

* salamshirween@gmail.com

Received: 26 February 2023 **Accepted: 12 May 2023**

DOI: https://doi.org/10.24237/ASJ.02.02.741C

Abstract

In this study, nanostructured $ZnNiCo_2O_4$ and $MnNiCo_2O_4$ electrodes were fabricated by spray pyrolysis method and annealed at 550°C for 2 h. The structural, optical, and Photoelectrochemical properties were studied. The structural properties were examined using X-ray diffraction (XRD). The results show that the samples have a cubic spinel structures. The atomic percentage determined by (EDX) and the thickness (cross-section) of films measured by (FE-SEM), as well as the surface roughness measured through (AFM) are all used for analysis. The optical properties were investigated by UV-visible spectrophotometer, and the energy band gaps of $ZnNiCo_2O_4$ and $MnNiCo_2O_4$ were estimated to be approximately 2.2 and 2.4 eV respectively. The photoelectrochemical, comprising of photocurrent density, linear sweep voltammograms (LSV), and Mott-Schottky (MS), displayed flat band values of (1.5 eV and -0.55 eV) Vs NHE for $ZnNiCo_2O_4$ and $MnNiCo_2O_4$ respectively, where the conduction band and valance band values of $ZnNiCo_2O_4$ were (C. B = -0.6 eV and V.B = 1.6 eV), while those of $MnNiCo_2O_4$ were (C.B= -0.65 eV and V.B= 1.75 eV). The corresponding photocurrent densities for $ZnNiCo_2O_4$ and $MnNiCo_2O_4$ were 35 μA/cm^2 and 50 μA/cm^2, respectively. The

electrodes were comprehensively studied for $ZnNiCo_2O_4$ and $MnNiCo_2O_4$ under a neutral water condition.

Keywords: Photoelectrochemical, Transition Metal Oxides, Photocatalytic, Spinel Structure.

تحضير بعض الأقطاب ذات تركيب الاسبنيل الرباعي للتطبيقات الفوتوكيميائية

عبدالسلام محمود حسن[1] و زياد طارق خضير[2] و عمار هادي جريز[3]

[1]المديرية العامة لتربية ديالى

[2] قسم الفيزياء - كلية العلوم - جامعة ديالى

[3] مركز بحوث النانو تكنولوجي والمواد المتقدمة - الجامعة التكنلوجية

الخلاصة

في هذا البحث، تم تحضير أقطاب $ZnNiCo_2O_4$ و $MnNiCo_2O_4$ النانوية التركيب بطريقة الرش بالانحلال الحراري وتم تلدينها عند درجة حرارة 550^oC ± لمدة ساعتين. تمت دراسة الخصائص التركيبية والبصرية والفوتوكيميائية, حيث تم فحص الخصائص التركيبية باستخدام حيود الأشعة السينية (XRD) وأظهرت النتائج أن العينات لها تركيب إسبنيل مكعب وتم حساب النسب الذرية بواسطة (EDX) وكذلك السمك (المقطع العرضي) بـواسطة (FE-SEM) وكذلك خشونة السطح باستخدام جهاز (AFM). تم فحص الخصائص البصرية بواسطة مقياس الطيف الضوئي المرئي للأشعة فوق البنفسجية، حيث كانت قيم فجوات الطاقة لكل من $ZnNiCo_2O_4$ و $MnNiCo_2O_4$ بحوالي 2.2 eV و 2.4 eV على التوالي. تمت دراسة المعلمات الفوتوكيميائية ، مثل كثافة التيار الضوئي و (LSV) و (Mott-Schottky), وتم حساب Flat Band من نتائج Mott-Schottky وكانت بحدود (1.5 eV and -0.55 eV) Vs NHE لأغشية $ZnNiCo_2O_4$ و $MnNiCo_2O_4$ على التوالي، وكانت قيم حزمة التوصيل وحزمة التكافؤ المحسوبة ايضاً من Mott-Schottky بحدود (C.B=-0.6 eV) و (V.B=1.6 eV) لغشاء $ZnNiCo_2O_4$ بينما كانت قيم حزمة التوصيل وحزمة التكافؤ ل $MnNiCo_2O_4$ (C.B= - 0.65 eV) و (V.B= 1.75 eV)وكانت كثافة التيار الضوئي لكل من $ZnNiCo_2O_4$ و $MnNiCo_2O_4$ بحدود 35 µA/cm^2 و 50µA/cm^2)على التوالي.

الكلمات المفتاحية: التطبيقات الفوتوكيميائية, أكاسيد المعادن الانتقالية، التحفيز الضوئي، تركيب الإسبنيل.

Introduction

The spinel structure of metal oxides has captivated the attention of materials scientists due to their exceptional physical and chemical features [1]. Investigating the decreased dimensionality of spinel-type metal oxides at the nanoscale has been conducted for a variety of applications, such as chemical gas sensors, High-capacity anode materials for Lithium-ion batteries, super-capacitors, pigments, catalysts, and spintronics [2]. The spinel structure has proven to be a particularly productive family of (MTMO) materials. Of particular interest is nickel cobaltite ($NiCo_2O_4$), which has been studied for its potential application in water electrolysis and oxygen evolution. The essential characteristics of spinel structures are highly contingent upon the precise distribution of cations occupying octahedral and tetrahedral sites in the cubic lattice of spinels. Despite their potential, these materials exhibit inadequate electrical conductivity. Different techniques like designing nano-architectures, compositing metal oxides with highly conductive polymers, and chemical substitution of Nobel metals were developed and demonstrated to drastically improve their electrochemical properties. Chemical substitution of metals in oxide nanostructures offers great promise for modulating electrochemical properties, as demonstrated by [3]. Mn-Ni-Co and Zn-Ni-Co oxides have also been identified as potential electrode materials due to their increased electrical conductivity and photoelectrochemical performance enhancement [4, 5]. In this study, we investigate the use of spinel cobaltites ($ZnNiCo_2O_4$, $MnNiCo_2O_4$) electrodes for photocatalytic applications, synthesized via the chemical spray pyrolysis (CSP) method.

Experimental Procedure

Nanostructured Cobaltite films ($ZnNiCo_2O_4$ and $MnNiCo_2O_4$) were deposited on a preheated FTO-coated glass substrate by using the spray pyrolysis method. The solutions are prepared using a mixture of Nickel nitrate ($Ni(NO_3)_2.6H_2O$), Cobalt nitrate ($Co(NO_3)_2.6H_2O$), Zinc nitrate ($Zn(NO_3)_2.6H_2O$) and Manganese acetate $Mn(CH_3COO)_2$ $.4H_2O$, all of 0.05 M. All the salts were dissolved in 100 ml distilled water, and a final solution was prepared by combining (Zn:Ni:Co) and (Mn:Ni:Co) solutions at a volumetric ratio of (0.5:0.5:2), and stirring the mixture for 20 minutes using a magnetic stirrer, resulting in a clear and homogeneous solution. The FTO-coated glass substrates were cleaned ultrasonically with ethanol and DIW followed by being dried at 80 ^{0}C for 30 min to eliminate the impurities remaining on the substrate. The spraying temperature was 400^{o}C, and the time of spray was 10 sec, the distance between the substrate to a nozzle was ±30cm, and the spray rate was 5 mL/min . The films were then annealed at a temperature of 550°C for 2 h, other parameters were detailed in Table 1. The deposited electrodes were characterized using X-ray diffraction (XRD) analysis with Cu-Kα radiation. The Atomic Force Microscope (AFM) was utilized to assess the roughness, root mean square, and average diameter of particles. The cross-section of the films and EDX were investigated using a Field emission scanning electron microscope (FE-SEM).

Table 1: Experimental parameters of spray pyrolysis deposition process.

PARAMETER	VALUE
Solution concentration	0.05 M
Volumetric ratio	0.5:0.5:2
Deposition temperature	400 ◦C
Annealing temperature	550 550 °C for 2 h
Distance between the substrate to a nozzle	30 cm
Spray rate	5 mL/min
Air pressure	1.5 bar

Photoelectrochemical Characterization

The cell of photocatalysis employs a three-electrode setup immersed in an aqueous electrolyte (Na_2SO_4), as depicted in Figure 1. This configuration consists of two active electrodes: a photoanode (Pt: Platinum wire) and a photocathode (film) as well as a third electrode (Ag/AgCl: Silver/silver chloride) serving as the reference electrode. The electrodes were immersed in an electrolyte solution of sodium sulfate Na_2SO_4 with a concentration of 0.5M. The tests were conducted at ambient temperature. The photo-current was measured by (DY2300 POTENTIOSTAT), at an applied potential of (-0.5 v). Linear sweep voltammetry (LSV) curves were recorded at a scan rate of 5 $mV.s^{-1}$.

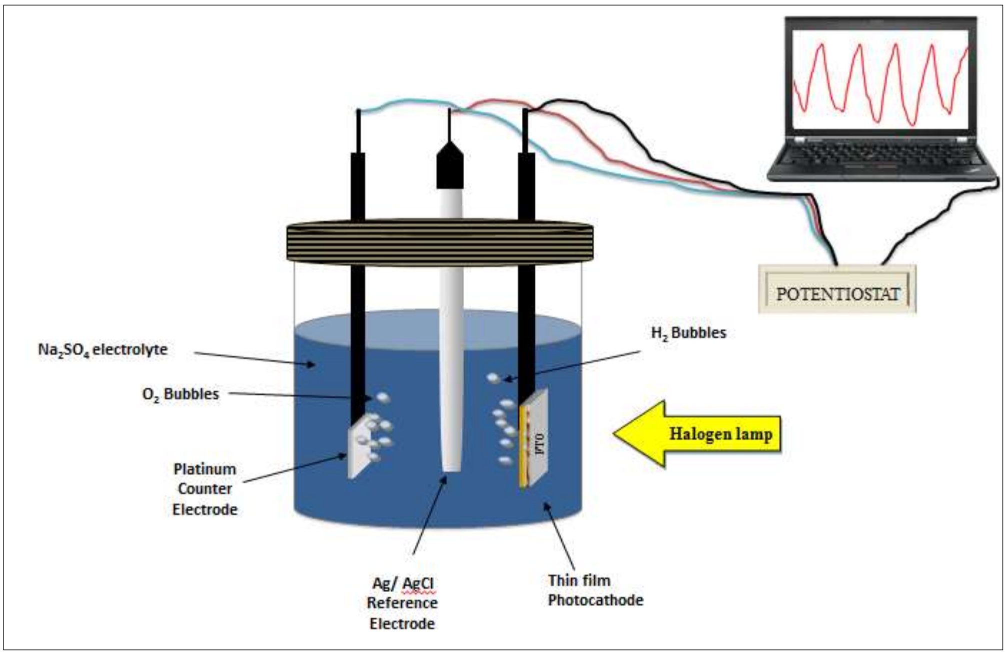

Figure 1: Diagram of Photoelectrochemical Cell.

Results and Discussion

Structure properties

Crystal structure

The spinel structures of Cobaltite films ($ZnNiCo_2O_4$, $MnNiCo_2O_4$) were presented in Figure 2, exhibiting the spinel crystal structure. The Tetrahedral (T_d) sites were occupied by Co ions while the Octahedral (O_h) sites were shared between (Ni and Zn or Mn) and Co. In the series $ZnNi_xCo_{2-x}O_4$ spinels, tetrahedral sites were occupied by the inactive Zn^{2+} to rule out their catalytic contributions, and emphasize the catalytically more active octahedral sites. Ni was employed as a substitute for octahedrally coordinated Co to facilitate the adjustable modification of electronic structure [6].

Academic Science Journal

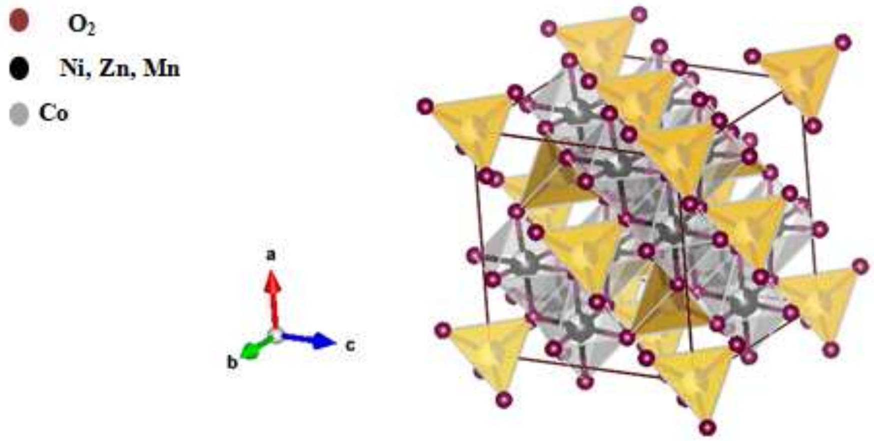

Figure 2: Spinel Structure of Cobaltites films. [Designed by Vesta app].

XRD measurements

The XRD pattern of synthesized films is shown in Figure 3. The XRD analysis indicated that the polycrystalline films were a pure phase and all samples confirm the formation of cubic spinel structure of Cobaltites films. The diffracted peaks of the quaternary spinel Cobaltites ($ZnNiCo_2O_4$ and $MnNiCo_2O_4$) are positioned at 31.4°, 36.9°, 54.5°, 59.4°, and 65.5°. The values match well with a cubic spinel structure standard ICDD file no.#73-1701 [7]. The diffraction peaks of spinel samples correspond to the (hkl) indices (220), (311), (422), (511) and (440), respectively.

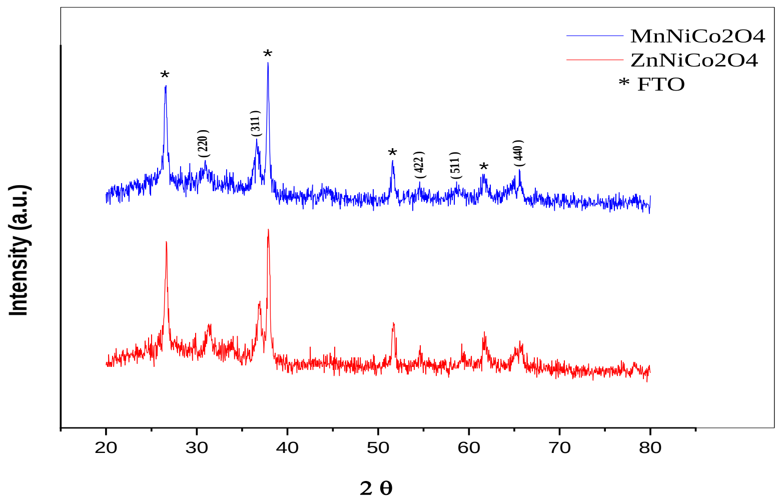

Figure 3: XRD patterns of $ZnNiCo_2O_4$ and $MnNiCo_2O_4$ films.

The average crystallite size of films is calculated using the Scherrer equation [8]:

$$D = \frac{0.9\lambda}{\beta cos\theta} \quad .... (1)$$

where D: The average crystallite size, λ: wavelength and β: full width at half maximum.

The average crystallite sizes of $ZnNiCo_2O_4$ and $MnNiCo_2O_4$ films are approximately (19.3 and 16.8) nm, respectively. The lattice parameters are shown in Table 2. The lattice parameters of the cubic lattice are determined from d spacing for the plane of (3 1 1) at the 2θ value of 36.9°and 36.7° of $ZnNiCo_2O_4$ and $MnNiCo_2O_4$ films respectively by using equation [9]:

$$\frac{1}{d^2_{hkl}} = \frac{h^2+k^2+l^2}{a^2} \quad ....(2)$$

where d is the interplanar spacing, and h, k, l are the Miller indices.

The results of the structure properties of Cobaltites films are in good agreement with the reported values of $ZnNiCo_2O_4$ [7, 9 and 10] and $MnNiCo_2O_4$ films [11].

Table 2: Crystallite sizes and lattice parameters of films**.**

SAMPLE	2Θ	FWHM	D_{AVG} (NM)	D_{311} (Å)	LATTICE CONSTANTS A=B=C (Å)	THE VOLUME OF UNITE CELL (NM^3)
$ZnNiCo_2O_4$	**36.9**	**0.434**	**19.3**	**0.2437**	**0.808**	**0.5281**
$MnNiCo_2O_4$	**36.7**	**0.496**	**16.8**	**0.2423**	**0.803**	**0.519**

FE-SEM measurements

The cross-section of Cobaltite films deposited at 400°C, and annealed at 550°C, was characterized by FE-SEM. As shown in Figures 4, the FE-SEM images indicate good grains growth. Variations in the grain size of $NiCo_2O_4$ are not only influenced by the preparation parameters, such as heat treatment, but also by the number of substituents (Zn, Mn) present in the parent matrix [12]. The EDX images of $ZnNiCo_2O_4$ and $MnNiCo_2O_4$ films are presented in Figure 5, and their atomic percentages are reported in Table 3.

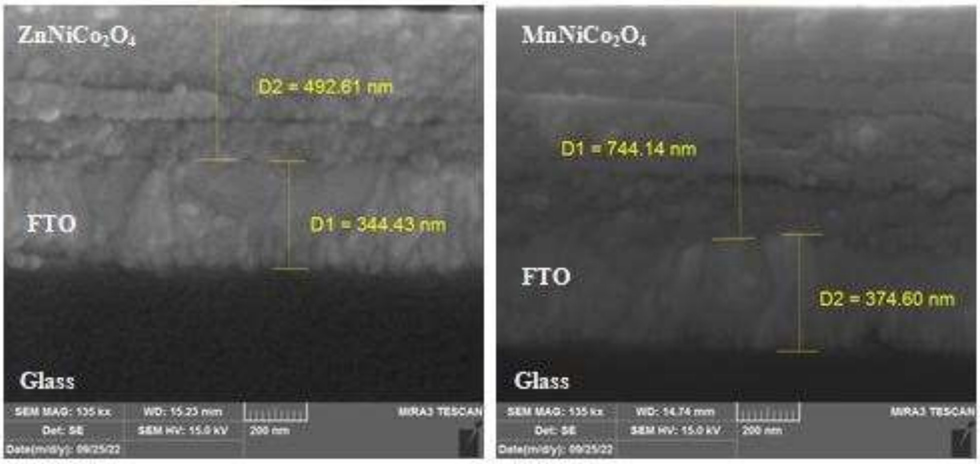

Figure 4: FE-SEM (Cross Section) of $ZnNiCo_2O_4$ and $MnNiCo_2O_4$ films.

Table 3: EDX atomic percent of $ZnNiCo_2O_4$ and $MnNiCo_2O_4$ films.

SAMPLE	O %	CO %	NI %	ZN %	MN %
$ZnNiCo_2O_4$	50.55	32.22	7.54	9.69	
$MnNiCo_2O_4$	60.86	27.53	6.75		4.86

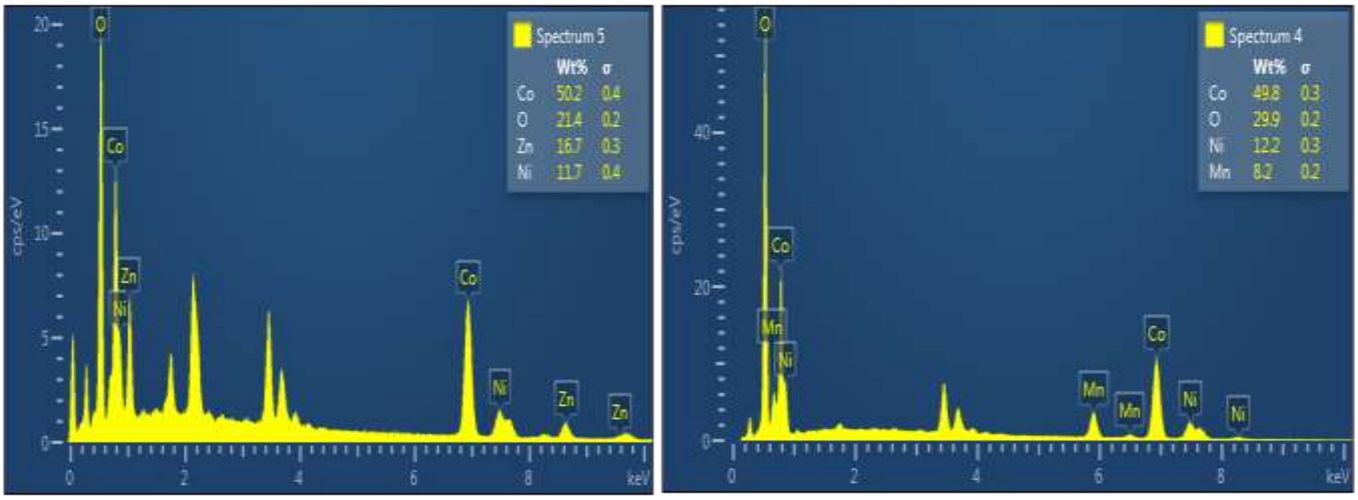

Figure 5: EDX images of $ZnNiCo_2O_4$ and $MnNiCo_2O_4$ films.

AFM measurements

The morphology of $ZnNiCo_2O_4$ and $MnNiCo_2O_4$ films was studied by atomic force microscopy (AFM). Figure 6 displays images of the surfaces depicting a uniform and homogenous growth

Academic Science Journal

on the substrate. Table 4 presents the average diameter, root mean square, and roughness average of Cobaltite films.

Table 4: AFM results of $ZnNiCo_2O_4$ and $MnNiCo_2O_4$ films.

SAMPLE	ROUGHNESS AVERAGE (NM)	RMS (NM)	AVERAGE DIAMETER (NM)
$ZnNiCo_2O_4$	**4**	**5.13**	**68.95**
$MnNiCo_2O_4$	**3.83**	**4.9**	**146.09**

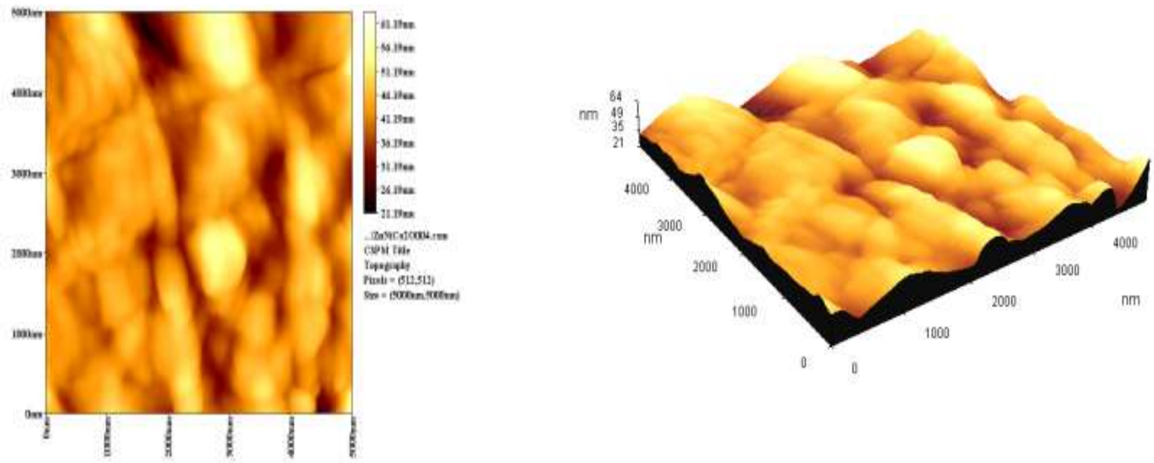

a) $ZnNiCo_2O_4$

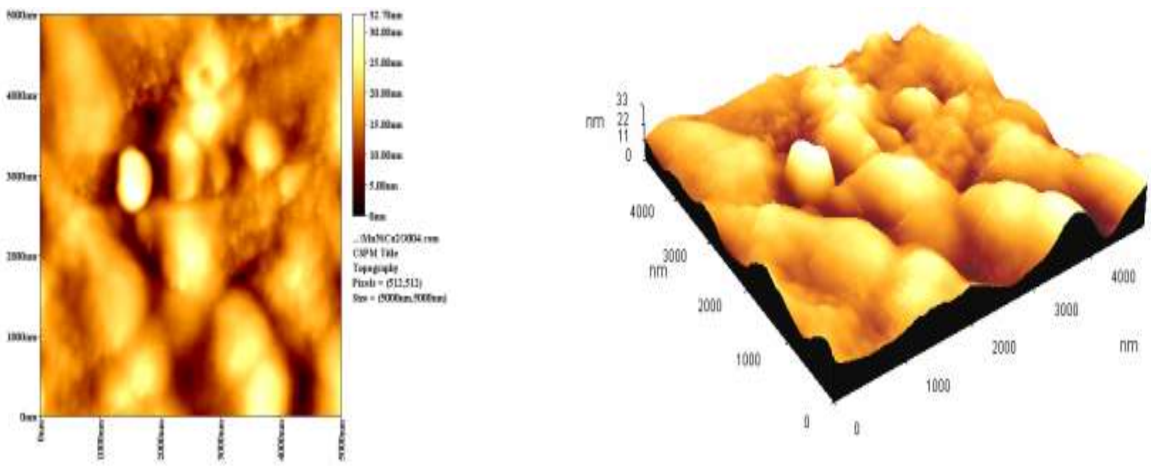

b) $MnNiCo_2O_4$

Figure 6: AFM images of: a) $ZnNiCo_2O_4$ b) $MnNiCo_2O_4$

Optical measurements

UV–visible absorption spectra of $ZnNiCo_2O_4$ and $MnNiCo_2O_4$ films in the wavelength range of 350–1000 nm were shown in Figure 7. The absorbance spectrum reveals that the films have considerable absorption across the entire visible range (350–1000 nm), indicating a strong absorption of most of the visible wavelengths. When compared to a solar spectrum, which has a notable intensity in the visible range, it suggests that these films are viable materials to be used as solar absorbers [13].

The energy band gap was determined by plotting $(\alpha.E)^2$ against the photon energy (E) of the films, as shown in Figure 7. The absorption edges of quaternary films in the Tauc plot cuts the abscissa at 2.2 eV and 2.4 eV for $ZnNiCo_2O_4$ and $MnNiCo_2O_4$ films respectively, which agrees well with the reported values of Cobaltites films [14], [15], [16]. The band-gap energy is determined using the equation [17].

$\propto h\upsilon = B_o (h\upsilon - Eg^{opt})^r$……….(3)

The band gap results in the films, allowing them to absorb all visible wavelengths in the range of visible region (400-1000 nm).

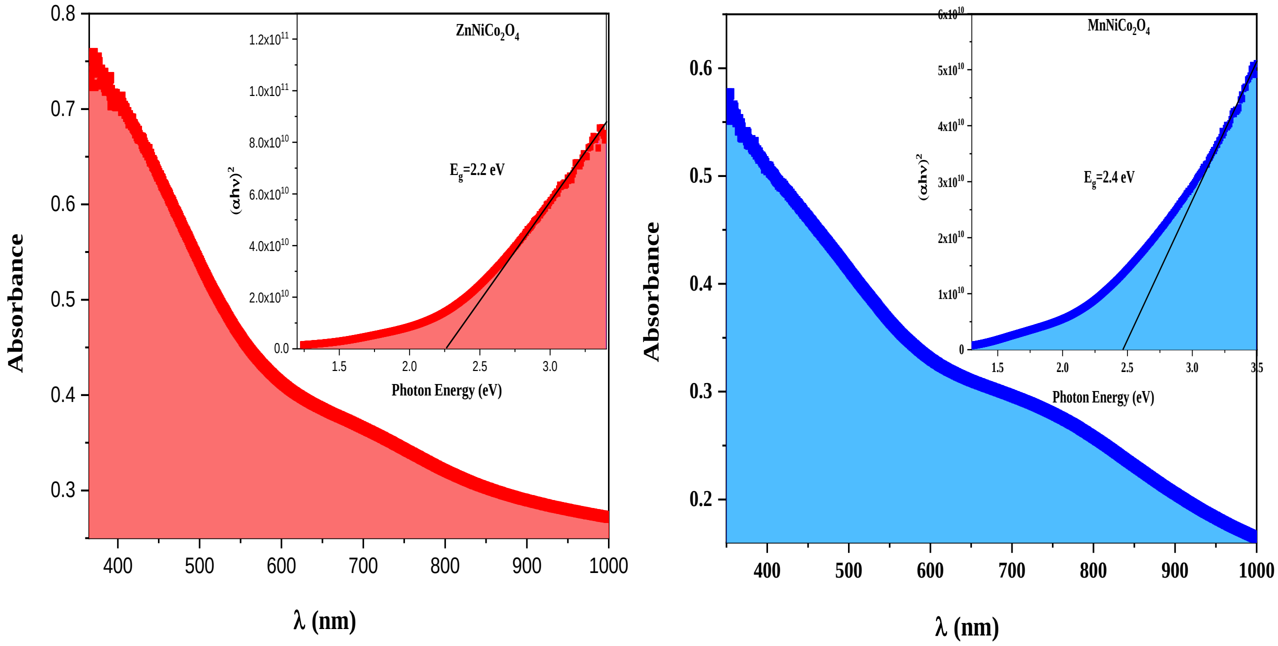

Figure7: UV–Vis Absorbance spectrums and Energy gaps of $ZnNiCo_2O_4$ and $MnNiCo_2O_4$ films.

Academic Science Journal

Characterization of Photocatalytic Activity

Linear sweep voltammetry (LSV)

The Photoelectrochemical (PEC) activity of Cobaltites electrodes was studied by using Photoelectrochemical cell, featuring a standard photoanode (Platinum wire as a counter electrode) and Ag/AgCl (Silver/Silver chloride) as reference electrode, whilst $ZnNiCo_2O_4$ and $MnNiCo_2O_4$ electrodes acted as the photocathodes. The results of current density were measured at a scan rate of 5 $mV.s^{-1}$ in Na_2SO_4 electrolyte with a concentration of 0.5 M. The light source was a 60-watt halogen lamp. Figure 8 presents the LSV of $ZnNiCo_2O_4$ and $MnNiCo_2O_4$ electrodes. At (-0.5 V), the films produced the highest photocurrent of 30 and 39 $\mu A/cm^2$ for $ZnNiCo_2O_4$ and $MnNiCo_2O_4$ respectively, indicating photocatalyst activity under illumination. The *I–V* curve displays a nonlinear behavior, which may be attributed to the Schottky barrier at the metal–semiconductor contacts [14].

Photoelectrochemical cells were used to analyze the photocurrent density stability of $ZnNiCo_2O_4$ and $MnNiCo_2O_4$ electrodes by switching off and on the light every 60 seconds. Figure 9 shows photocurrent density curves of nanostructured electrodes, which exhibit PEC activity with the photocurrent densities of (35 and 50) $\mu A/cm^2$ at -0.5 V for $ZnNiCo_2O_4$ and $MnNiCo_2O_4$ respectively.

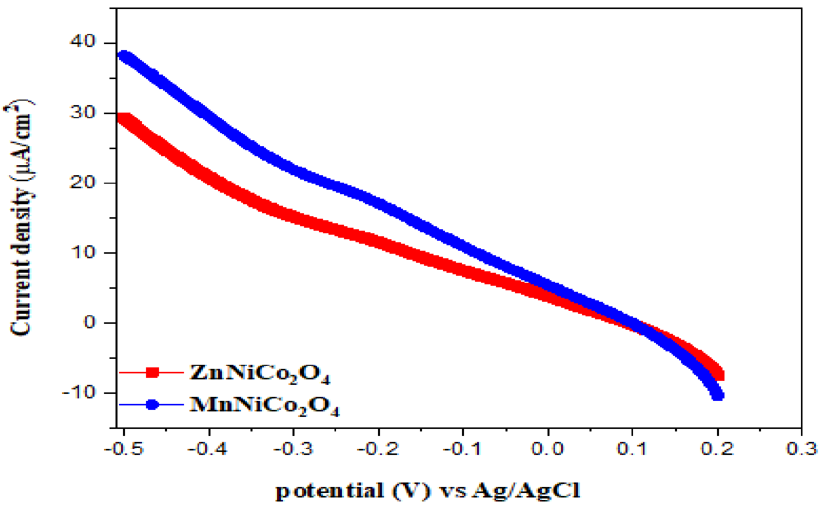

Figure 8: Linear Sweep Voltammograms (LSV) of $ZnNiCo_2O_4$ and $MnNiCo_2O_4$ Electrodes.

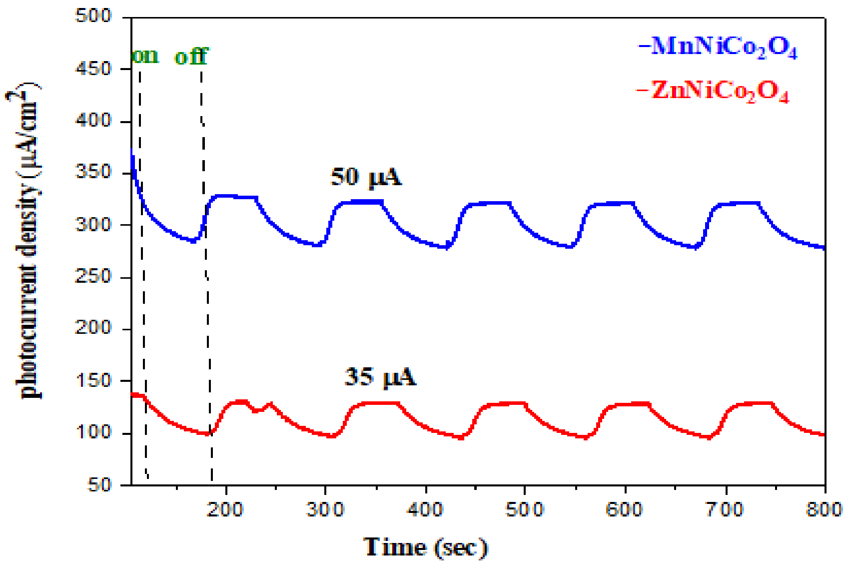

Figure 9: Photocurrent densities of $ZnNiCo_2O_4$ and $MnNiCo_2O_4$ Electrodes.

Band structure

The flat band potential (E_{fb}) is a crucial parameter for assessing the performance of photoelectrodes, and can be used to estimate the positions of band edges in new materials [18]. The flat band potential is a fundamental factor that gives information that allows the estimation of the conduction band edge potential at the surface of the semiconductor [19]. The flat-band potential values were determined from the Mott-Schottky plot presented in Figure 10. The flat-band potentials of electrodes were calculated from the x-intercept of the linear region. The curves illustrated that the behaviors of the electrodes are p-type (negative slope) and n-type (positive slope) with flat band values of (1.5 V and -0.55 V) vs. NHE for $ZnNiCo_2O_4$ and $MnNiCo_2O_4$ respectively. The conduction band and valance band values of $ZnNiCo_2O_4$ and $MnNiCo_2O_4$ electrodes were found to be (C.B= -0.6 eV and V.B= 1.6 eV) and (C.B= -0.65 eV and V.B= 1.75 eV) respectively. The general relation between electrode capacitance (C) and applied voltage value (E) for n-type and p-type semiconductors is described by the following form of the Mott-Schottky equation (4) [19]:

$$\frac{1}{C^2} = \frac{2}{\varepsilon\varepsilon o A^2 qNq}\left(-E + EFB + \frac{KBT}{q}\right) \ldots\ldots\ldots\ldots(4)$$

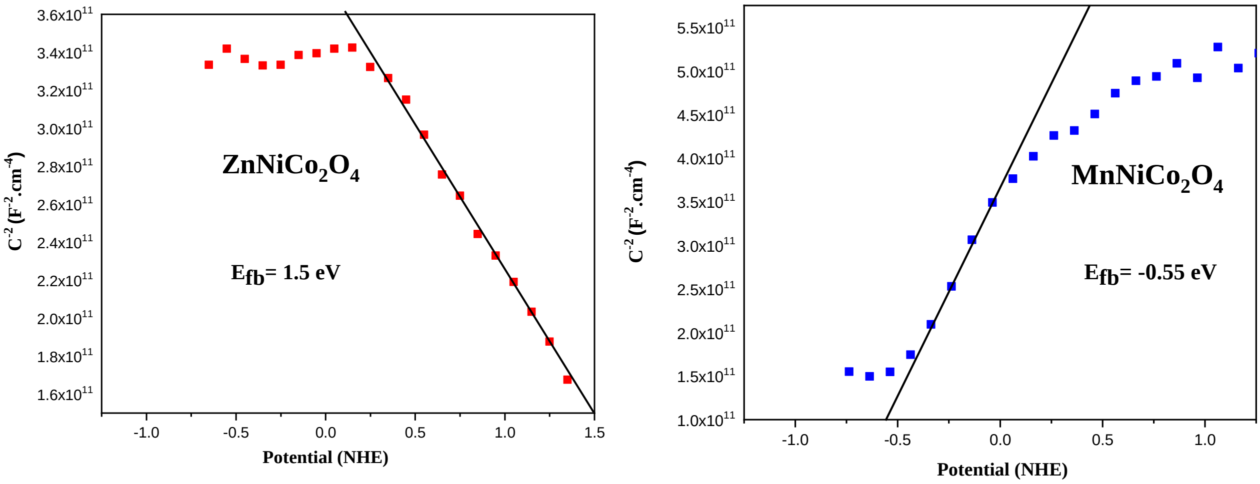

Figure 10: Flat band potential of $ZnNiCo_2O_4$ and $MnNiCo_2O_4$ electrodes.

This study is the first to systematically investigate the photocatalytic properties of $ZnNiCo_2O_4$ and $MnNiCo_2O_4$ Cobaltite electrodes using photocurrent, LSV, and flat band potential determination techniques in photoelectrochemical systems.

Conclusion

Nanostructured cobaltite electrodes were deposited onto FTO-coated glass substrates via spray pyrolysis, followed by annealing at 550ºC for two hours. The structural study revealed that the electrodes have a spinel structure. The nanocrystalline grain surface morphology was observed from (AFM), and the atomic percent was calculated by field emission scanning electron micrograph images (FE-SEM). UV–vis absorption spectra of glass samples exhibited that the films had a good absorption with a band gap of (2.2 and 2.4 eV) for $ZnNiCo_2O_4$ and $MnNiCo_2O_4$ respectively. The electrodes exhibited good PEC activity in terms of photocurrent density at a scan rate 5 mV/s, while Mott-Schottky measurements revealed p-type and n-type behavior of the flat-band potential. The conduction band and valance band values for $ZnNiCo_2O_4$ were (C. B= -0.6 eV and V.B= 1.6 eV), while those of $MnNiCo_2O_4$ were (C.B= -0.65 eV and V.B= 1.75 eV). These findings make Cobaltite electrodes suitable for the fabrication of heterojunctions for photocatalytic applications.

References

1. E. R. Kumar, R. Jayaprakash, G. S. Devi, P. S. P. Reddy, Synthesis of Mn substituted CuFe2O4 nanoparticles for liquefied petroleum gas sensor applications, Sens. Actuators B, 191, 186–191(2014)
2. J. Kumar, C. R. Mariappan, V. Kumar, S. Murugavel, G. V. Prakash, Study of spinel-type ZnNixCo2-xO4 nano-particles, synthesised by thermal decomposition of ternary metal nitrate solutions, Materials Research Bulletin, 83, 632–639(2016)
3. M. S. Tamboli, D. P. Dubal, S. S. Patil, A. F. Shaikh, V. G. Deonikar, M. V. Kulkarni, N. N. Maldar, A. M. Asiri Inamuddin, P. Gomez-Romero, B. B. Kale, D. R. Patil, Mimics of microstructures of Ni substituted Mn1-xNixCo2O4 for high energy density asymmetric capacitors, Chemical Engineering Journal, 307(1), 300-310(2017)
4. Q. Zhang, High-performance hybrid supercapacitors based on self-supported 3D ultrathin porous quaternary Zn-Ni-Al-Co oxide nanosheets. Nano Energy, 28, 475-485(2016)
5. C. Wu, Fabrication of Cobalt-Nickel-Zinc Ternary Oxide Nanosheet and Applications for Supercapacitor Electrode. Frontiers in chemistry, 6, 597 (2018)
6. W. Ting, J. Wang, Y. Sun, Y. Duan, S. Sun, X. Hu, S. Xi, Y. Du, C. Wang, Z. J. Xu., Origin of Electronic Structure Dependent Activity of Spinel ZnNixCo2-xO4 Oxides for Complete Methane Oxidation, Applied Catalysis B: Environmental, 256(5), (2019).
7. V. Kumar, V. Gajraj, K.I. Gnanasekar, S. Dsoke, S. Indris, H. Ehrenberg, B. Roling, C.R. Mariappan, Hybrid aqueous supercapacitors based on mesoporous spinel-analogous Zn-Ni-Co-O nanorods: Effect of Ni content on the structure and energy storage, Journal of Alloys and Compounds, 882, 160712(2021)
8. S. A. Hameed, N. A. Bakr, A. M. Hassan, A. N. Jasim, Structural and optical properties of Cu_2ZnSnS_4 films fabricated by chemical spray pyrolysis, AIP Conference Proceedings, 2213, 020082(2020)
9. W. Deeloed, W. Wattanathana, P. Jantaratana, P. Prompinit, S. Wannapaiboon , S. Singkammo, S. Sattayaporn, A. Laobuthee, S. Suramitr, Y. Hanlumyuang, A systematic

variation in cationic distribution and its influence on the magnetization of mixed-metal (nickel and zinc) cobaltite spinels, Mater. Res. Express, 7,096104(2020)

10. J. Kumar, C. R. Mariappan, V. Kumar, S. Murugavel, G. V. Prakash, Study of spinel-type ZnNixCo2-xO4 nano-particles, synthesised by thermal decomposition of ternary metal nitrate solutions, Materials Research Bulletin, 83, 632–639(2016)

11. TAREKEGN HELISO DOLLA, Synthesis and Characterization of Mixed Transition Metal Oxides and their Composites with Carbon for Energy Storage Applications**,** Doctoral Thesis, University of Johannesburg, Johannesburg, (2017)

12. M. M. Munir, A. R. Khan, G. M. Mustafa, S. K. Abbas, M. A. Raza, S. Atiq, S. Naseem, Dielectric and magnetic variance in $NiCo_2O_4$ spinels mediated by Zn-substitution for efficient data and energy storage, Applied Physics A, 127(492), (2021)

13. X. Chen, S. Cai, E. Yu, J. Li, J. Chen, H. Jia, Photothermocatalytic performance of ACo 2 O 4 type spinel with light-enhanced mobilizable active oxygen species for toluene oxidation, Appl. Surf. Sci., 484, 479–488(2019)

14. L. Hu, L. Wu, M. Liao, X. Fang, High Performance NiCo2O4 Nano film Photodetectors Fabricated by an Interfacial Self-Assembly Strategy**,** Adv. Mater., 23,1988–1992(2011)

15. A. Bashir, Low temperature, solution processed spinel NiCo2O4 nanoparticles as efficient hole transporting material for mesoscopic n-i-p perovskite solar cells, Sol. Energy, 196, 367–378(2020)

16. Zhibin Wu, Yirong Zhu, Xiaobo Ji**,** NiCo2O4-based Materials for Electrochemical Supercapacitor**,** J. Mater. Chem. A, 2, 14759-14772(2014)

17. Z. T. Khodair, M. A. Al-Jubbori, A. M. Hassan, M. S. Aljuboori, F. I. Sharrad **,** Structural Properties of ($Sn_{1-x}Mg_xO$) Thin Films and Optical Parameter Dependence with Gamma Ray Irradiation**,** J. Electron. Mater., 48(1), (2019)

18. A. Hankin, F. E. Bedoya-Lora, J. C. Alexander, A. Regoutz, G. H. Kelsall, Flat band potential determination: avoiding the pitfalls**,** J. Mater. Chem. A,7, 26162–26176 (2019)

19. E. Wlaźlak, J. Kalinowska-Tłuścik, W.Nitek, S. Klejna, K. Mech, W. Macyk, K.Szacilowski, Triiodide organic salts: photoelectrochemistry at the border between insulators and semiconductors**,** Chem Electro Chem, 5, 3486-3497(2018)